

January 2014

## A MODIFIED C-DUMP CONVERTER FOR PMSM MACHINE USED IN A FLYWHEEL ENERGY STORAGE SYSTEM

K. GOPI

JNTU, Anantapur, k.gopi@gmail.com

E. RAMAKRISHNA

JNTU, Anantapur, e.ramakrishna@gmail.com

K. NARASIMHAIAH ACHARI

J.N.T.U.A, Anantapur, chari.narasimhaiah@gmail.com

G. KISHORE

J.N.T.U.A, Anantapur, gudipatikishor@gmail.com

Follow this and additional works at: <https://www.interscience.in/ijeee>



Part of the [Power and Energy Commons](#)

---

### Recommended Citation

GOPI, K.; RAMAKRISHNA, E.; ACHARI, K. NARASIMHAIAH; and KISHORE, G. (2014) "A MODIFIED C-DUMP CONVERTER FOR PMSM MACHINE USED IN A FLYWHEEL ENERGY STORAGE SYSTEM," *International Journal of Electronics and Electrical Engineering*: Vol. 2 : Iss. 3 , Article 4.

Available at: <https://www.interscience.in/ijeee/vol2/iss3/4>

This Article is brought to you for free and open access by Interscience Research Network. It has been accepted for inclusion in International Journal of Electronics and Electrical Engineering by an authorized editor of Interscience Research Network. For more information, please contact [sritampatnaik@gmail.com](mailto:sritampatnaik@gmail.com).

# A MODIFIED C-DUMP CONVERTER FOR PMSM MACHINE USED IN A FLYWHEEL ENERGY STORAGE SYSTEM

K.GOPI, E. RAMAKRISHNA, K. NARASIMHAIAH ACHARI & G. KISHORE

JNTU, Anantapur

**Abstract** - This paper presents a modified C-dump converter for permanent magnetic synchronous (PMSM) machine used in the flywheel energy storage system. The converter can realize the energy bidirectional flowing and has the capability to recover the energy extracted from the turnoff phase of the PMSM machine. The principle of operation, modeling, and control strategy of the system has been investigated in the paper. Simulation and experimental results of the proposed system are also presented and discussed.

**Keywords** - permanent magnetic synchronous (PMSM) machine, c-dump converter, flywheel energy storage system.

## I. INTRODUCTION

The flywheel energy storage system (FESS) is an attractive option for temporary energy storage in high power utility applications and hybrid electric systems [1], [2]. The permanent magnet synchronous machine (PMSM) is one of the suitable motors for the FESS [3]. The common half-bridge topology for high-speed PMSM is shown in Fig. 1. It includes a buck chopper and a half-bridge converter. Compared with the full-bridge converter, the half bridge converter has half the number of switches and avoids the short circuit across the phase leg in the full-bridge converter.

However, this half-bridge topology has two disadvantages for the FESS: 1) the energy unidirectional flow, and 2) the energy of the turnoff phase is consumed on the resistance which means the waste of energy. In order to overcome these drawbacks, a modified C-dump converter for high-speed PMSM used in the FESS is presented in this paper. The principle of operation and the analysis of the proposed converter are developed.

## II. STRUCTURE AND PRINCIPLE

Fig. 2 shows the modified C-dump converter for PMSM used in the FESS. The proposed converter includes a half-bridge converter (switches  $T_a, T_b, T_c$ ), an energy recovery chopper (switch  $T_r$ ; diodes  $D_1, D_2, D_3, D_r$ ; inductance  $L_r$  and capacitor  $C_0$ ), a bidirectional DC-DC converter (switches  $T_1, T_2$ ; inductance  $L_2$  and capacitor  $C_3$ ), and a DC filter (Inductance  $L_1$  and capacitors  $C_1, C_2$ ).  $U_1$  stands for the source and  $R$  stands for the load.

The modified converter has two working modes: the FESS charging mode and the FESS discharging mode. In the FESS charging mode, the source supplies energy to the flywheel, therefore  $S_1$  is on and  $S_2$  is off. In this mode, the half-bridge converter works in the motor operation.  $T_a, T_b$ , and are operated with the duration of 120 electrical degrees.

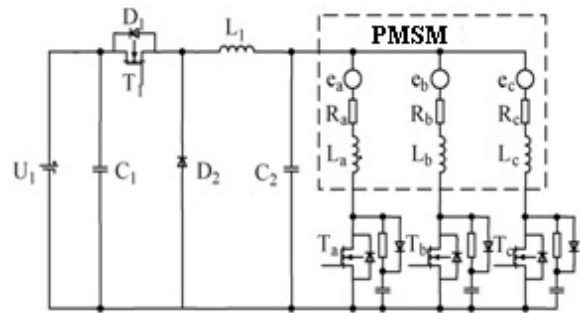


Fig.1 : Common half-bridge topology for high-speed PMSM.

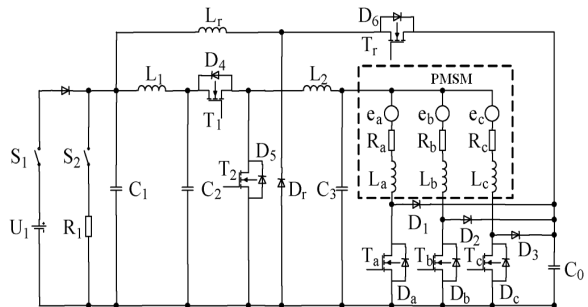


Fig.2 : Modified C-dump converter for the FESS.

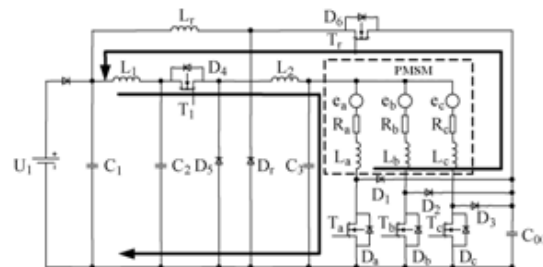


Fig. 3. Modified converter working in the charging mode

$T_r$  works in the pulse width modulation (PWM) operation mode and recovers the energy of the turnoff phase to the source [4]. The bidirectional DC-DC converter works in buck operation mode ( $T_1$  works in PWM operation mode and  $T_2$  is off.) to control the motor speed. Fig. 3 illustrates the modified converter for the FESS working in the charging mode. In the FESS discharging mode, the PMSM (with flywheel) acts as a generator to

discharge the kinetic energy of the flywheel into the load, therefore  $S_1$  is off and  $S_2$  is on. In this

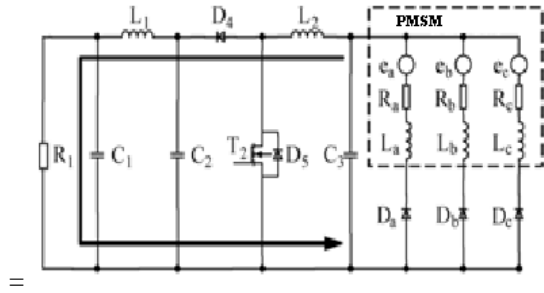


Fig. 4 : Modified converter working in the discharging mode.

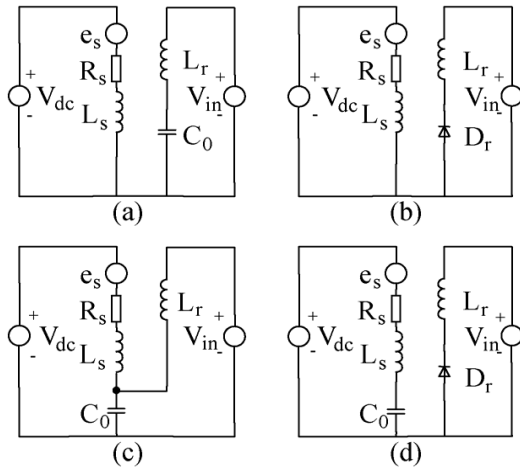


Fig. 5 : The equivalent circuits of the converter in its switching operation. (a)  $T_s$  on,  $T_r$  on; (b)  $T_s$  on,  $T_r$  off; (c)  $T_s$  off,  $T_r$  on; (d)  $T_s$  off,  $T_r$  off.

mode, the half-bridge converter acts as a diode rectifier to convert the high-frequency AC to the DC. are all off and form a diode rectifier. With the speed of flywheel decreasing, the output voltage drops. In order to keep the output voltage stable, the bidirectional DC-DC converter works in boost operation mode ( $T_2$  works in PWM operation mode and  $T_1$  is off). Fig. 4 illustrates the modified converter for the FESS working in the discharging mode.

### III. MODELING AND CONTROL STRATEGY

The modeling and analysis of the proposed converter are presented in this part.

#### A. Dynamic Model

Four distinct modes of operation can be identified for the proposed converter in the charging mode. The equivalent circuits of the converter in its switching operation are shown in Fig. 5. The voltage drop of the switch and the diode, the resistance of the inductance, and the mutual inductance of the motor phases are ignored.  $T_s$  considers as  $T_a$ , or  $T_b$ , or  $T_c$ .  $V_{dc}$  is the bus voltage (voltage of the capacitor  $C_3$ ),  $e_s$  is the back-electromotive force (back-EMF) of the

motor,  $R_s$  is the motor phase resistance,  $L_s$  is the motor phase inductance,  $i_s$  is the motor phase current,  $V_{co}$  is the capacitor  $C_o$  voltage,  $V_{in}$  is the source input voltage (voltage of the capacitor  $C_1$ ),  $L_r$  is the energy recovery circuit inductance,  $i_r$  is the current of the energy recovery inductor  $L_r$ , and  $k_o$  is the buck factor.

1)  $T_s$  on,  $T_r$  on

$$V_{dc} = L_s \frac{di_s}{dt} + e_s + R_s i_s \quad (1)$$

$$V_{in} = V_{co} - L_r \frac{di_r}{dt} \quad (2)$$

$$C_o \frac{dV_{co}}{dt} = -i_r \quad (3)$$

$$V_{dc} = k_o V_{in} \quad (4)$$

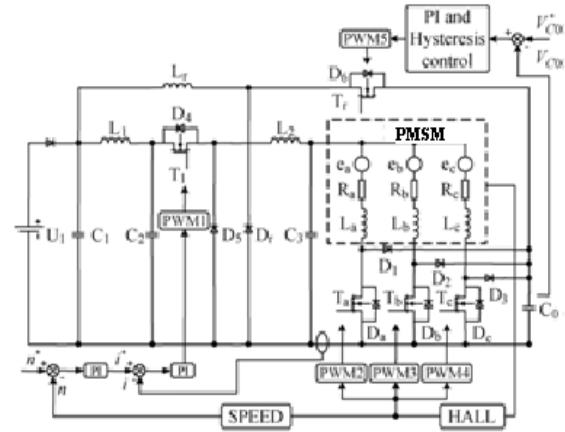


Fig. 6. Control structure of the converter in the charging mode.

2)  $T_s$  on,  $T_r$  off

$$V_{dc} = L_s \frac{di_s}{dt} + e_s + R_s i_s \quad (5)$$

$$V_{in} = -L_r \frac{di_r}{dt} \quad (\text{if } i_r > 0) \quad (6)$$

$$V_{co} = \text{constant} \quad (7)$$

$$V_{dc} = k_o V_{in} \quad (8)$$

3)  $T_s$  off,  $T_r$  on

$$V_{dc} = L_s \frac{di_s}{dt} + e_s + R_s i_s + V_{co} \quad (9)$$

$$V_{in} = V_{co} - L_r \frac{di_r}{dt} \quad (10)$$

$$C_o \frac{dV_{co}}{dt} = i_s - i_r \quad (11)$$

$$V_{dc} = k_o V_{in} \quad (12)$$

4)  $T_s$ , off,  $T_r$ , off

$$V_{dc} = L_s \frac{di_s}{dt} + e_s + R_s i_s + V_{co} \quad (13)$$

$$V_{in} = -L_r \frac{dir}{dt} \quad (\text{if } i_r > 0) \quad (14)$$

$$C_o \frac{dV_{co}}{dt} = i_s \quad (15)$$

$$V_{dc} = k_o V_{in} \quad (16)$$

## B. Design of the Main Parameter

The main parameters of the proposed converter are derived as follows.

### 1) Energy Extracted From the Turnoff Phase:

The system works in steady state and the switching loss is ignored. The energy extracted from the turnoff phase can be described as

$$W_{LS} = \frac{1}{2} L_s i_{smax}^2 \quad (17)$$

Where is the energy extracted from the turnoff phase. is the motor phase current in commutation moment; it can be

TABLE 1

RATINGS AND PARAMETERS OF PMSM

Rated voltage (V)	100
Rated stator current (A)	20
Rated power (kW)	2
Frequency (Hz)	5333
Phase inductance (mH)	0.06
Phase resistance ( $\Omega$ )	0.2

Obtained from (1). The power extracted from the turnoff phase is

$$P_{LS} = \frac{W_{LS}}{t} = 3 \times \frac{1}{2} L_s i_{smax}^2 \frac{1}{T} = \frac{3}{2} L_s i_{smax}^2 \frac{np}{60} \quad (18)$$

Where  $n$  is the speed of the motor and is the pairs of poles.

### 2) Energy recovery capacitor $C_o$ :

The energy extracted from the turnoff phase is delivered to the energy recovery capacitor.

Therefore

$$W_{LS} = \frac{1}{2} L_s i_{smax}^2 = \frac{1}{2} C_o [(V_{co} + \Delta V_{co})^2 - V_{co}^2] \quad (19)$$

$$C_o = \frac{L_s i_{smax}^2}{(V_{co} + \Delta V_{co})^2 - V_{co}^2}$$

Where  $\Delta V_{co}$  is the voltage variation of the capacitor. The voltage  $V_{co}$  should be higher than  $V_{dc} + e_s$ .

### 3) Energy Recovery Inductance:

According to energy conservation, the energy recovered to source can be described

As

$$\begin{aligned} \frac{1}{2} L_s i_{smax}^2 &= \frac{1}{2} C_o [(U_c + \Delta U_c)^2 - U_c^2] \\ &= \frac{1}{2} L_r i_{rMAX}^2 - \frac{1}{2} L_r i_{rMIN}^2 \end{aligned} \quad (21)$$

Where  $i_{rMAX}$  ( $i_{rMIN}$ ) is the maximum (minimum) current of the inductance  $L_r$ . In order to keep the energy recovery fast, the  $L_r$  should not be too large. Therefore, it is better for the  $L_r$  to working discontinuous conduction mode  $i_{rMIN}=0$

$$\frac{1}{2} L_s i_{sMAX}^2 = \frac{1}{2} L_r i_{rMAX}^2 \quad (22)$$

$$L_r = \frac{L_s i_{rMAX}^2}{i_{rMAX}^2} \quad (23)$$

## C. Control Strategy

The control structure of the modified converter working in the charging mode is shown in Fig. 6. It includes the motor speed control and the recovery capacitor voltage control. The motor speed control includes double loops: the inner current loop and the outer speed loop. The commutation of phases is decided based on the output of three Hall effect sensors. The motor phases are protected against over current. The proportional-integral (PI) control combined with the hysteresis control is used in capacitor  $C_o$  voltage control. It is recommended for the converter due to its small voltage fluctuation of the energy recovery capacitor and current ripple of the motor.

## IV. SIMULATION AND EXPERIMENT

To verify the performance of the proposed converter, simulations and experimental tests have been performed. The ratings and parameters of the PMSM are presented in Table I. Parameters of the converter are shown in Table II.

TABLE II

PARAMETERS OF THE CONVERTER

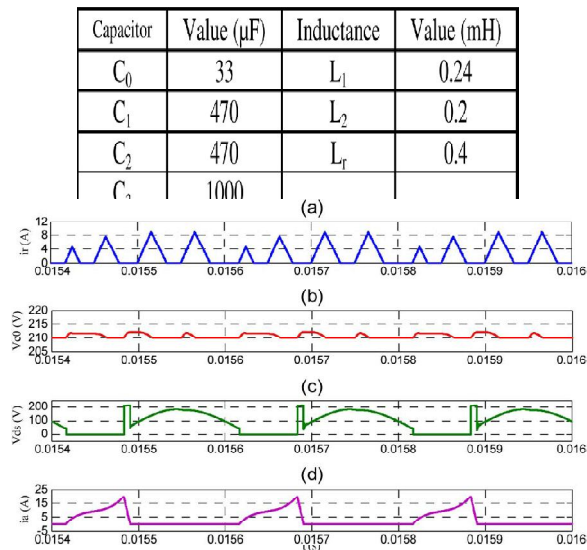


Fig.7. Simulation results of the converter working in the charging mode. a) Recovery current. (b) Voltage of the capacitor  $C_0$ . (c) voltage between the drain and the source of the MOSFET (phase A). (d) Current of the phase A.

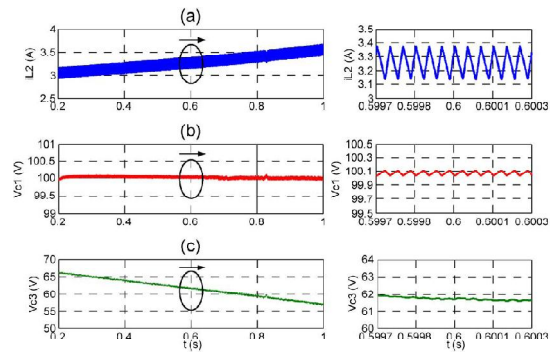


Fig.8. Simulation results of the converter working in the discharging mode. (a) Current of inductance  $L_2$ . (b) Output voltage of the converter. (c) Output voltage of the PMSM rectified by the diode rectifier.

A. Simulation Results

Fig. 7 shows the simulation results of the proposed converter working in the charging mode. At this range, the peak value of the phase current is about 21 A, as shown in Fig. 7(d). Fig. 7(a) shows the recovery current which is limited to a peak value of 9 A. Fig. 7(b) shows the voltage of energy recovery capacitor which stays around 210 V, and increases to 213 V during commutation when the capacitor starts to discharge into the source. Fig. 7(c) shows the voltage ( $V_{ds}$ ) between the drain and the source of the metal-oxide-semiconductor field-effect transistor (MOSFET), which equals to the phase terminal voltage plus the bus voltage ( $V_{dc}$ ).

Fig. 8 shows the simulation results of the proposed converter working in the discharging mode. Fig. 8(a) shows the current of inductance  $L_2$ . Fig. 8(b) shows the output voltage of the converter (voltage of the capacitor  $C_1$ ) which stays around 100 V

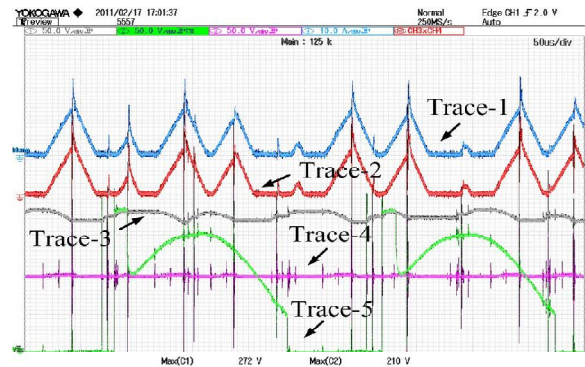


Fig. 9. Experimental results of the converter working in the charging mode when the average bus current is 15.6 A. (1) Recovery current  $i_r$ . (2) Recovery power. (3) Voltage of  $C_0$ . (4) Source input voltage. (5) Voltage between the drain and the source of the MOSFET.

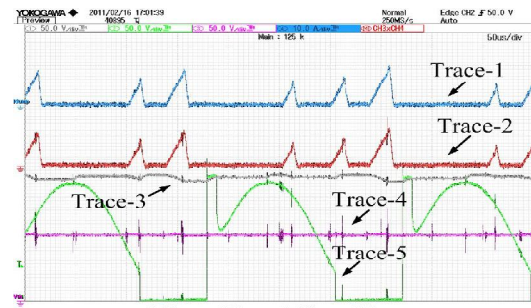


Fig. 10. Experimental results of the converter working in the charging mode when the average bus current is 8.2 A. (1) Recovery current  $i_r$ . (2) Recovery power. (3) Voltage of  $C_0$ . (4) Source input voltage. (5) Voltage between the drain and the source of the MOSFET.

When the flywheel speed decreases, Fig. 8(c) shows the output voltage of the PMSM rectified by the diode rectifier (voltage of the capacitor  $C_3$ ).

B. Experimental Results

Fig. 9 shows the experimental results of the converter working in the charging mode when the average bus current (current of the inductance  $L_2$ ) is 15.6 A. Waveform “1” shows the recovery current which is similar to what was observed in simulation. Waveform “4” shows the source input voltage (voltage of the capacitor  $C_1$ ). Waveform “2” is the product of waveforms “1” and “4” which equals to the recovery power. It is about 387 W. Waveform “3” shows the voltage of energy recovery capacitor  $C_0$ . A small charging and discharging action of the capacitor can be seen from the waveform, and the average voltage of

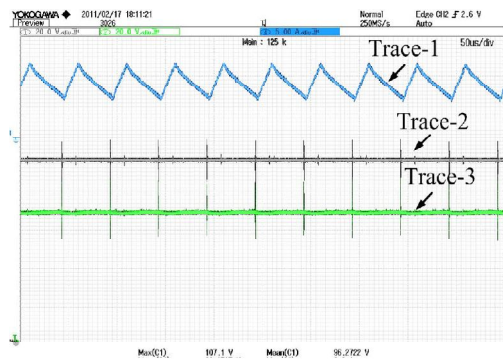


Fig. 11. Experimental results of the converter working in the discharging mode when the output voltage of the PMSM is 70 V. (1) Current of inductance (50  $\mu$ s/div, 5 A/div). (2) Output voltage of the converter (50  $\mu$ s/div, 20 V/div). (3) Voltage of the capacitor (50  $\mu$ s/div, 20 V/div).

$C_0$  the voltage between the drain and the source of the MOSFET. Fig. 10 shows the experimental results of the converter working in the charging mode when the average bus current is 8.2 A. With the phase current decreasing, the recovery energy reduces. The average recovery current is 1.48 A, and the average recovery power is about 145.9 W.

Fig. 11 shows the experimental results of the converter working in the discharging mode when the output voltage of the PMSM rectified by the diode rectifier is 70 V. Waveform “1” shows the current of

inductance  $L_2$ . Waveform “2” shows the output voltage of the converter which is stable, about 96.2V. Waveform “3” is the voltage of the capacitor  $C_3$ .

## V. CONCLUSION

This paper has presented a modified C-dump converter for PMSM used in the FESS. The proposed converter can realize the bidirectional energy flowing and has the capability to recover the energy extracted from the turnoff phase which is useful for the motor driver system especially for the FESS. The principle of operation, modeling, and control strategy of the system has been presented. Simulation and experiment validate the theoretical results and demonstrate the good performance of the converter. The study indicates that the converter is suitable for the FESS applications.

## REFERENCES

- [1] M. M. Flynn, P. McMullen, and O. Solis, “Saving energy using flywheels,” *IEEE Ind. Appl. Mag.*, vol. 14, no. 6, pp. 69–76, Nov./Dec. 2008.
- [2] C. W. Lu, “Torque controller for brushless DC motors,” *IEEE Trans. Ind. Electron.*, vol. 46, no. 2, pp. 471–473, Apr. 1999.
- [3] R. Krishnan and S. Lee, “PM Brushless dc motor drive with a new power converter topology,” *IEEE Trans. Ind. Appl.*, vol. 33, pp. 973–982, July/Aug. 1997.

